Neural control of rapid binocular eye movements: Saccade-vergence burst neurons

Julie Quinet[a,1], Kevin Schultz[a], Paul J. May[b,c,d], and Paul D. Gamlin[a]

[a]Department of Ophthalmology and Visual Sciences, University of Alabama at Birmingham, Birmingham, AL 35294; [b]Department of Neurobiology and Anatomical Sciences, University of Mississippi Medical Center, Jackson, MS 39216; [c]Department of Ophthalmology, University of Mississippi Medical Center, Jackson, MS 39216; and [d]Department of Neurology, University of Mississippi Medical Center, Jackson, MS 39216

Edited by Martin S. Banks, University of California, Berkeley, CA, and approved September 24, 2020 (received for review July 21, 2020)

During normal viewing, we direct our eyes between objects in three-dimensional (3D) space many times a minute. To accurately fixate these objects, which are usually located in different directions and at different distances, we must generate eye movements with appropriate versional and vergence components. These combined saccade-vergence eye movements result in disjunctive saccades with a vergence component that is much faster than that generated during smooth, symmetric vergence eye movements. The neural control of disjunctive saccades is still poorly understood. Recent anatomical studies suggested that the central mesencephalic reticular formation (cMRF), located lateral to the oculomotor nucleus, contains premotor neurons potentially involved in the neural control of these eye movements. We have therefore investigated the role of the cMRF in the control of disjunctive saccades in trained rhesus monkeys. Here, we describe a unique population of cMRF neurons that, during disjunctive saccades, display a burst of spikes that are highly correlated with vergence velocity. Importantly, these neurons show no increase in activity for either conjugate saccades or symmetric vergence. These neurons are termed saccade-vergence burst neurons (SVBNs) to maintain consistency with modeling studies that proposed that such a class of neuron exists to generate the enhanced vergence velocities observed during disjunctive saccades. Our results demonstrate the existence and characteristics of SVBNs whose activity is correlated solely with the vergence component of disjunctive saccades and, based on modeling studies, are critically involved in the generation of the disjunctive saccades required to view objects in our 3D world.

saccades | vergence | binocular control | neural recordings | oculomotor

When viewing objects at a given distance, we make rapid, saccadic eye movements in which the two eyes move conjugately (1). When shifting gaze between targets located at different distances along the midline, we employ much slower, symmetric vergence eye movements in which the two eyes rotate in equal, but opposite, directions (1). However, the vast majority of normal eye movements shift gaze between targets located at different distances and eccentricities in three-dimensional (3D) space. To acquire such targets, we generate disjunctive saccades, which are produced by the two eyes generally rotating in the same direction, but by different amounts, depending on target distance (1–3) (Fig. 1). Under normal viewing conditions, disjunctive saccades are, by far, the most commonly generated eye movements.

Despite their obvious importance, we do not yet understand the mechanisms underlying the production of disjunctive saccades. Currently, it is not known whether disjunctive saccades are produced solely by the vergence system, by the saccadic system, or through the combined action of both circuitries. Theoretical models based on behavioral studies have been developed to explain the neural control of disjunctive saccades. One model from Zee et al. (4) suggested that omnipause neurons, which gate the activity of saccadic burst neurons (SBNs), might also gate the activity of a putative population of saccade-vergence burst neurons (SVBNs). These SVBNs would be active during disjunctive saccades, such that the output of SVBNs sums with that of vergence velocity neurons (VVNs) to significantly increase vergence velocity during disjunctive saccades (5). In a modification of this model, Busettini and Mays (6) proposed that the saccadic burst from SBNs and a vergence motor error signal interact multiplicatively at SVBNs to produce a burst of activity solely during disjunctive saccades. A striking feature of these models is the proposal that a unique population of SVBNs exists that is active only during disjunctive saccades and is inactive during conjugate saccades or symmetric vergence movements. However, to our knowledge, no such class of cell has previously been reported in prior recording studies.

Prior recording experiments have demonstrated vergence position cells that discharge with a tonic firing rate as a function of the vergence angle in the supraoculomotor area (SOA), dorsal and lateral to the oculomotor nucleus (OMN) (7–9). These cells do not respond during conjugate saccades. A second class of vergence cells, VVNs, has been recorded with a similar distribution to vergence positon cells (7). Their activity correlates with vergence velocity during symmetric vergence movements but saturates above a vergence velocity of ∼30 deg/s (7), and so only accounts for ∼8% of the observed vergence velocity during disjunctive saccades (10). Experimental strabismus in monkeys results in disconjugate eye movements with widespread activity changes in the oculomotor system (11, 12), and specific changes in the activity of the SOA and cerebellar neurons that encode the inappropriate vergence angle that primates with strabismus develop (13, 14). Consequently, the understanding of the control of

Significance

Currently, it is not known whether disjunctive saccades, the eye movements generated when viewing objects in three-dimensional space, are produced solely by the vergence system, the saccadic system, or through some as-yet-undescribed neural circuitry. Here, we report the existence of a population of saccade-vergence burst neurons (SVBNs) in the central mesencephalic reticular formation that encode vergence velocity. They respond only during disjunctive saccades, and not during conjugate saccades or pure vergence movements, and their existence had been predicted by modeling studies. Our findings indicate that SVBNs are not only involved in the generation of disjunctive saccades, but they are the critical element for producing vergence changes at the speeds observed during disjunctive saccades.

Author contributions: J.Q., P.J.M., and P.D.G. designed research; J.Q., K.S., and P.D.G. performed research; J.Q. and K.S. analyzed data; and J.Q., K.S., P.J.M., and P.D.G. wrote the paper.

The authors declare no competing interest.

This article is a PNAS Direct Submission.

[1]To whom correspondence may be addressed. Email: juliequinet@gmail.com.

First published November 2, 2020.

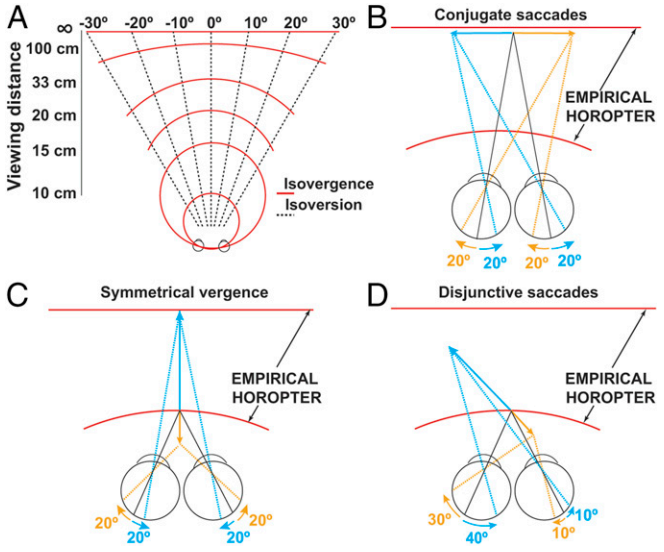

Fig. 1. Schematic describing symmetrical vergence, conjugate saccades, and disjunctive saccades. *A* shows the geometric case for movements that are either conjugate—all those made along isovergence lines, or symmetrical vergence—all those made along isoversion lines. *B–D* show these movements in a more real-world situation in which empirical studies have found that the horopter is significantly flatter than predicted geometrically (60, 61). The movements in depth in these panels are exaggerated for the purposes of clarity. *B* shows conjugate saccades for fixation at a distance where the empirical horopter is flat [~1 m in most individuals (60, 61)]. Note that both eyes move equally in the same direction. *C* shows vergence eye movements between targets on the midline at different distances. Note that both eyes move equally in opposite directions. *D* shows two examples of the vast majority of eye movements that are normally made between targets at different distances and eccentricities. Note that the required movements of the left and right eye are unequal. These are predominantly achieved through disjunctive eye movements that combine saccades with vergence (2, 3).

disjunctive saccades will be essential to explain and advance treatments for strabismus.

Other studies have suggested that the saccadic premotor pathway provides both the conjugate and the vergence premotor commands required to facilitate vergence velocity during disjunctive saccades (15, 16). Neural recordings of excitatory burst neurons in the paramedian pontine reticular formation (PPRF) during disjunctive saccades revealed that the firing of these premotor SBNs is correlated with one eye or the other (17), so they not only carry saccade-related information, but also potentially the vergence-related information necessary for disjunctive saccades (18). However, these models cannot readily explain the disjunctive saccade signals seen on medial rectus motoneurons (MRMNs), since all authorities agree that abducens internuclear interneurons (AINs) do not carry the appropriate signal from the SBNs in the PPRF to contralateral MRMNs (19, 20). Consequently, we turned our attention to the cMRF because it not only supplies input to MRMNs, it also innervates the preganglionic Edinger–Westphal nucleus (EWpg) (21–23). This nucleus contains motoneurons that control lens accommodation and pupillary constriction, which, along with vergence, are components of the near response. Given the evidence that neurons within the cMRF play a role in both horizontal saccadic eye movements (24–26) and the near response (21–23, 27), we hypothesized that the cMRF likely contained SVBNs critical for the control of disjunctive saccades. A brief report of this work has appeared in abstract form (28).

Results

We used MRI guidance and a neuronavigation system (Brainsight, Rogue Research) to direct single-unit recordings to the midbrain of two alert, trained rhesus monkeys. Recordings were performed in the range of 0 to 5 mm lateral to the OMN. The results described below are based on records from 18 SVBNs that were isolated in the cMRF lateral to OMN.

SVBNs. All identified SVBNs were active during either convergence or divergence disjunctive saccades, and remained silent during both near and far symmetric vergence eye movement, as well as during conjugate saccades. Overall, half of the recorded cells increased their firing rate for convergence disjunctive saccades, while half increased their firing rate for divergence disjunctive saccades.

Fig. 2 shows an example of an SVBN that discharges during either a leftward (Fig. 2*A*) or rightward (Fig. 2*B*) disjunctive saccade. Fig. 2*A* shows the behavior of this SVBN during a leftward disjunctive saccade in which the convergence velocity exceeded 150°/s and the horizontal position of the right eye changed 2.9°, while that of the left eye changed only 0.3°. Moreover, Fig. 2*B* shows the behavior of this cell during a rightward disjunctive saccade in which the convergence velocity again exceeded 150°/s, but the horizontal position of the right eye changed 0°, while that of the left eye changed 4.2°. Thus, even though the direction of the convergence disjunctive saccade is in the opposite direction in these two panels, the SVBN nevertheless discharges similarly with activity closely correlated with convergence velocity. In addition, this convergence SVBN was inactive during rightward or leftward divergence disjunctive saccades (Fig. 2 *C* and *D*), and did not discharge during smooth, symmetrical convergence eye movements (Fig. 2*E*) or during conjugate saccades (Fig. 2*F*). This behavior is unlike that of the other cell classes described previously in cMRF studies. Most previously described cMRF cells discharged for contraversive conjugate saccades (24, 26). In contrast, this SVBN increases its firing rate for both rightward and leftward disjunctive saccades, indicating a lack of tuning for a preferred horizontal direction.

One-half of the recorded SVBNs responded only during divergence disjunctive saccades, as shown in Fig. 3. In this example, during a leftward disjunctive saccade in which the divergence velocity exceeded 50°/s and the horizontal position of the left eye changed 2.9°, while that of the right eye changed only 0.2°, there is a robust discharge of the SVBN (Fig. 3*C*). Moreover, Fig. 3*D* shows the behavior of this cell during a rightward disjunctive saccade in which the divergence velocity again exceeded 50°/s, but the horizontal position of the left eye changed 1.2°, while that of the right eye changed 4.6°. Thus, even though the direction of the divergence disjunctive saccade is in the opposite direction in these two panels, the SVBN nevertheless discharges similarly with activity closely correlated with divergence velocity. In addition, this divergence SVBN was inactive during convergence disjunctive saccades (Fig. 3 *A* and *B*), and did not discharge during either smooth, symmetrical divergence eye movements (Fig. 3*E*) or during conjugate saccades (Fig. 3*F*).

SVBN Activity Is Unrelated to Vergence Angle. Vergence position cells in the SOA are characterized by a tonic firing rate that correlates with the vergence angle (8, 9). In contrast, our results demonstrate that the firing rate of SVBNs is unrelated to either the tonic convergence or tonic divergence angle. Specifically, there is no tonic activity in these cells during either symmetrical convergence (Fig. 2*E*) or divergence (Fig. 3*E*) movements and there is no tonic activity once they have been completed, and the vergence angle is maintained during fixation (Figs. 2 *A–E* and 3 *A–E*).

SVBN Activity Encodes Vergence Velocity. To examine whether SVBNs dynamically encode vergence velocity during disjunctive saccades, we tested the relationship between firing rate and vergence velocity of SVBNs. For the example of a convergence SVBN

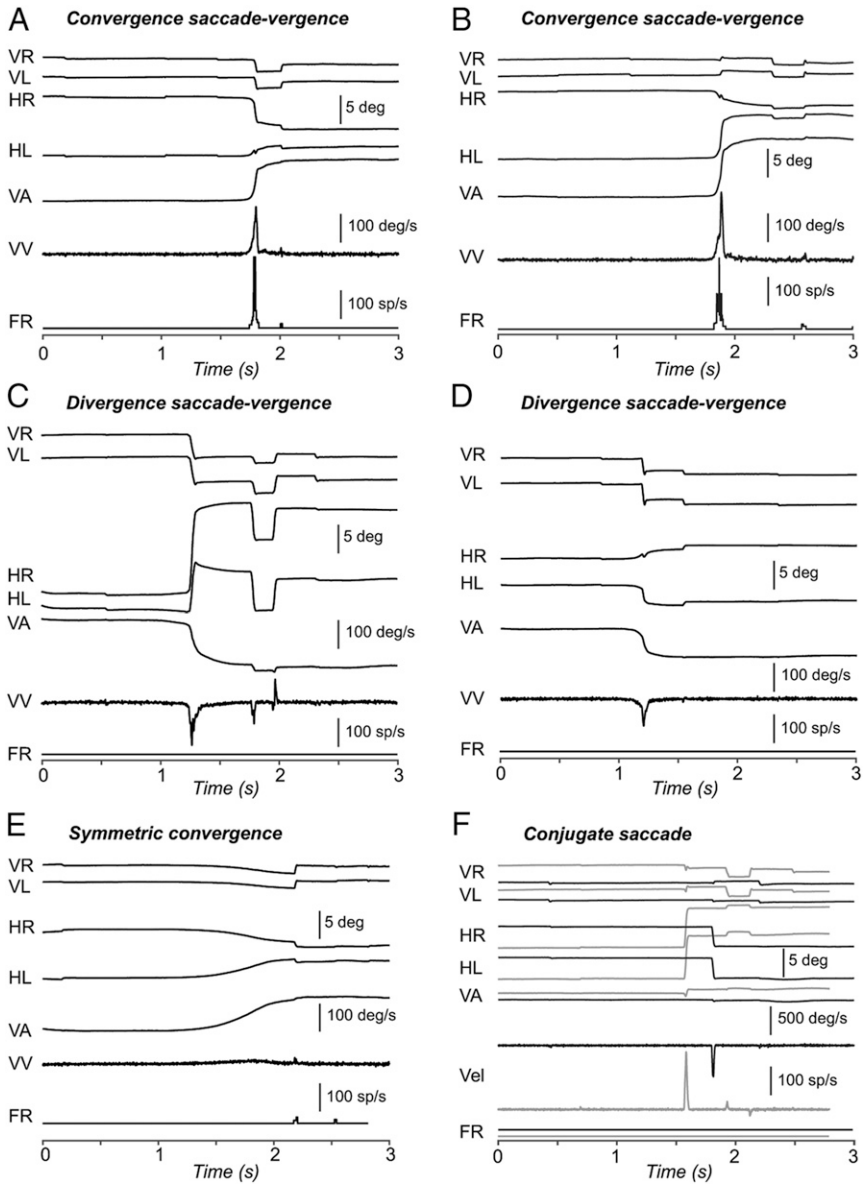

Fig. 2. Convergence saccade-vergence burst neuron (SVBN) discharging only for convergence disjunctive saccades (*A* and *B*) (C6 in Table 1). No discharge is present for divergence disjunctive saccades (*C* and *D*), symmetrical convergence eye movement (*E*), or for conjugate saccades (*F*). For conjugate saccades (*F*), the black lines represent leftward movements; the gray lines represent rightward movements. FR, firing rate; HL, horizontal left eye position; HR, horizontal right eye position; VA, vergence angle; Vel, version velocity; VL, vertical left eye position; VR, vertical right eye position; VV, vergence velocity. Positive values of horizontal eye movements correspond to the rightward direction, and negative values, to leftward directions. Positive values of vertical eye movements correspond to upward directions, and negative values, to downward directions. A positive-going vergence angle value indicates convergence.

shown in Fig. 2, firing rate clearly increased as a function of increases in convergence velocity (Fig. 4*A*). Moreover, no statistical correlation was observed between version velocity and the firing rate of this cell, independent of the direction of the saccade (Fig. 4*B*). The same result was observed for the example of a divergence SVBN shown in Fig. 3. The firing rate increases as a function of increases in divergence velocity (Fig. 4*C*). Furthermore, no statistically significant correlation was observed between the firing rate and version velocity of the disjunctive saccades (Fig. 4*D*).

In all 18 cases, the linear relationship between vergence velocity and firing rate had a significant Pearson correlation coefficient. To further define the characteristics of the SVBNs, we tested their response using different models, with particular attention to what signals were relevant. In a previous study (29), the activity of cMRF cells was tested by the following polynomial model equation: $\mathrm{FR}(t) = a + b\mathrm{LE}(t) + c\mathrm{RE}(t) + d\mathrm{LE}v(t) + e\mathrm{RE}v(t)$, where $\mathrm{FR}(t)$ is the instantaneous firing rate; a, b, c, d, and e are constants; and $\mathrm{LE}(t)$, $\mathrm{RE}(t)$, $\mathrm{LE}v(t)$, and $\mathrm{RE}v(t)$ represent the instantaneous left eye (LE) and right eye (RE) positions and velocities, respectively. By varying the parameters (constants), this model can represent monocular, version, or vergence signals. The use of a nonparametric bootstrap process (20, 30) allowed the determination of which eye-dependent terms could be eliminated or replaced with conjugate terms by checking for overlap of the confidence intervals (CIs) of parameters *b*–*e*, as determined by the bias corrected and accelerated method. Overlap of the eye position CIs, for example, would mean that they could be replaced with version signals, without changing the variance accounted for (VAF). In the previously studied group of

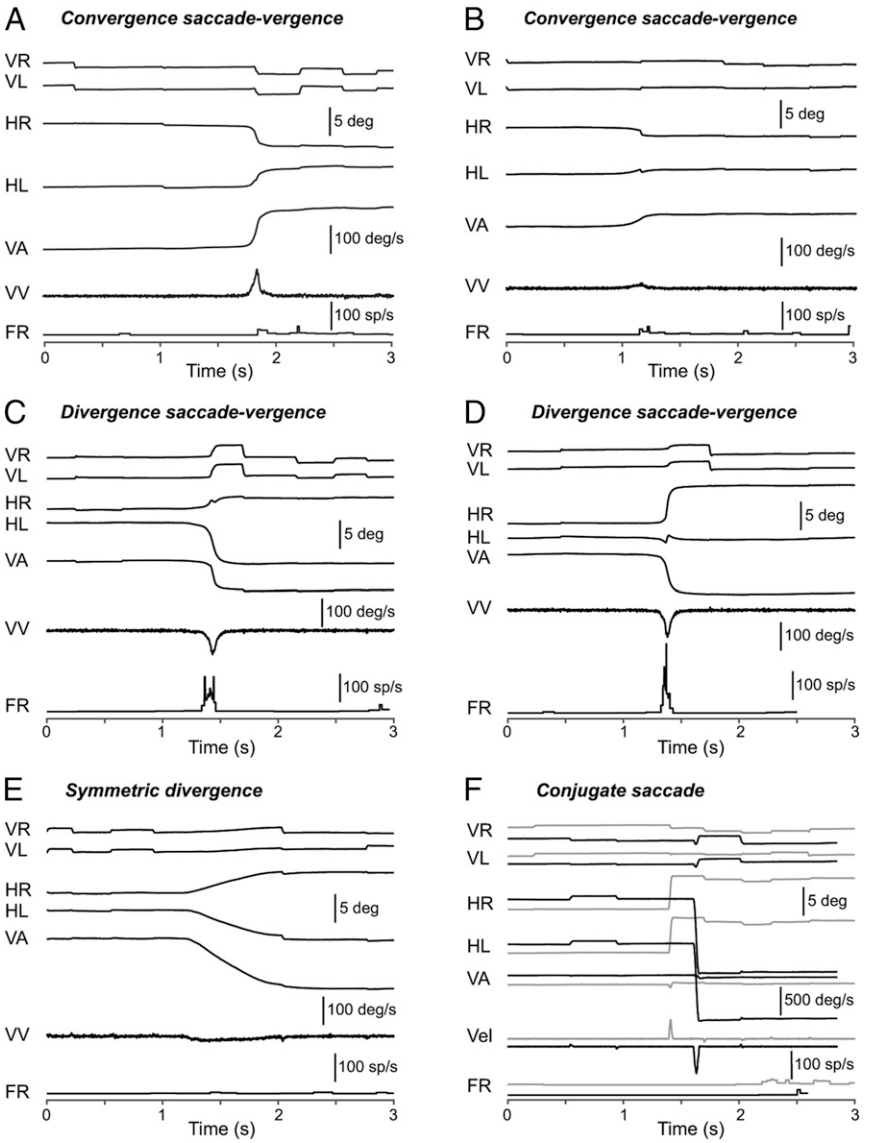

Fig. 3. Divergence saccade-vergence burst neuron (SVBN) discharging only for divergence disjunctive saccades (*C* and *D*) (D3 in Table 1). No discharge is present for convergence disjunctive saccades (*A* and *B*), for symmetrical divergence eye movement (*E*), or for conjugate saccades (*F*). For conjugate saccades (*F*), the black lines represent leftward movements, and the gray lines represent rightward movements. FR, firing rate; HL, horizontal left eye position; HR, horizontal right eye position; VA, vergence angle; Vel, version velocity; VL, vertical left eye position; VR, vertical right eye position; VV, vergence velocity. Eye movement conventions are as in Fig. 2.

cMRF cells, the left and right eye position terms could not be replaced by a single conjugate term and the velocity terms were eliminated (as they overlapped with zero). This led Waitzman et al. (29) to conclude that the discharges of cMRF cells were best explained in a monocular context. Using the same model and analysis for the population of SVBNs, with an identical bootstrap approach, the results were strikingly different. In every cell, the 95% CIs of both the position and velocity terms for the left eye and right eye overlapped with opposite sign. When left and right eye positions and velocities of each eye were replaced by vergence position and velocity terms, the VAF was not significantly changed compared to the model that included all monocular terms, validating this approach. In 10 of the 18 cells, vergence position overlapped with zero and could be eliminated. In the remaining cells, the maximum contribution by vergence position to the VAF was only 0.01 ± 0.01%, except for one cell (C2) in which the contribution was 4%. This was likely due to nonlinearities in the firing rate of this cell, since this contribution was effectively eliminated by a nonlinear fit (see below). Therefore, only the results of the linear model: $\mathrm{FR}(t) = a + bVV(t)$ are reported, giving a sensitivity value that can easily be compared against other cell populations. This model, which employs only vergence velocity, tightly predicts the firing rate with an $R^2 = 0.80 \pm 0.16$. The sensitivity values for convergence SVBNs are 1.1 ± 0.55 spikes·s^{-1}·deg^{-1}·s^{-1}, and for divergence SVBNs are 1.06 ± 0.62 spikes·s^{-1}·deg^{-1}·s^{-1}, with a population sensitivity of 1.09 ± 0.57 spikes·s^{-1}·deg^{-1}·s^{-1} (Table 1).

As has been reported for SBNs (31), the firing rate of some SVBNs exhibited saturation characteristics at higher velocities with less of an increase in activity required to generate a given increase in vergence velocity. So, in addition to a linear model, we also report the results of fitting to an asymptotic model: $\mathrm{FR}(t) = FRmax \times \left(1 - e^{-VV/C}\right)$, where *FRmax* is the peak firing rate of the cell and *C* is a constant. *FRmax* was set to a maximum

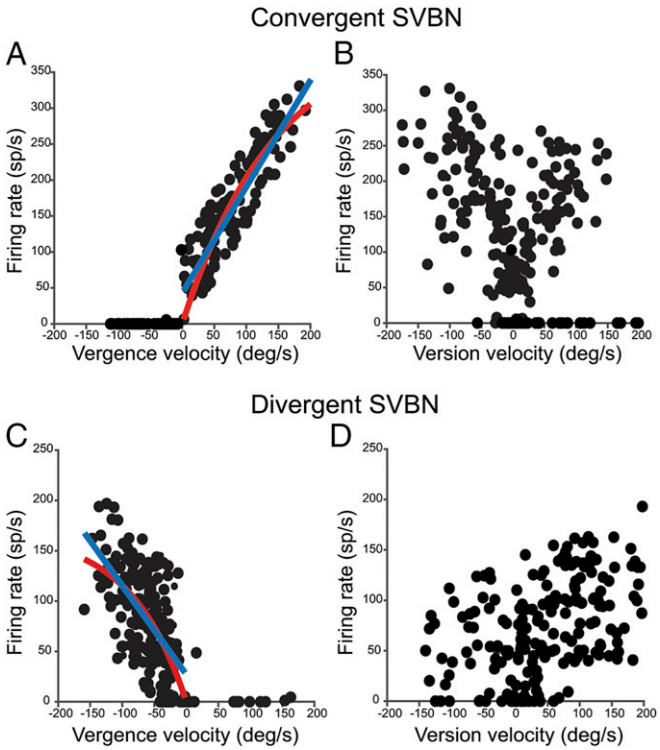

Fig. 4. Velocity firing rate relationships in SVBNs. Graphs demonstrate the relationship between vergence velocity during disjunctive saccades and firing rate (*A* and *C*), and between version velocity of the disjunctive saccades and firing rate (*B* and *D*) for a convergence SVBN (C6) (*A* and *B*) and a divergence SVBN (D3) (*C* and *D*). Positive and negative values of velocity are for convergence and divergence eye movements, respectively. The curve fitting (red trace) between the maximum firing rate and vergence velocity use the relationship: $FR(t) = FRmax \times (1 - e(-VV/C))$, where *VV* represent vergence velocity. Firing rates were tightly related to vergence velocity, but not conjugate velocity. The linear relationship between vergence velocity and firing rate is represented by the blue trace.

of 800 spikes/s and *C* was optimized (Table 1). In addition to this model, terms for left and right eye velocities, version velocity, version position, and vergence position were also computed, but as none impacted the fit values in a statistically significant manner, they were abandoned.

The same analysis was also performed to analyze trials with conjugate saccades and smooth symmetrical eye movements. No obvious trend existed in the data when comparing firing rate to horizontal conjugate velocity (e.g., Figs. 2*F* and 3*F*). For all SVBNs, the Pearson correlation was not significant for either horizontal directions (leftward and rightward) of conjugate saccades. In addition, there was no relationship between firing rate and vergence velocity during smooth symmetrical vergence eye movements in almost all cells. Only for cells C5, D2, and D5 was the Pearson correlation significant for symmetric divergence vs. firing rate. However, there was no clear trend in the data for these cells, so a linear model was applied, yielding an R^2 of <0.01, <0.01, and 0.04, respectively. This indicates that any correlation, if it does exist, is very weak.

SVBN Activity Leads Disjunctive Saccades. Based on the lag required for the best fit between firing rate and vergence velocity, the burst of activity during disjunctive saccades leads vergence velocity in recorded SVBNs (Table 1). The average lead time for convergence SVBNs was 35.7 ± 27.2 ms while that for divergence SVBNs was 25.2 ± 25.1 ms with a population average lead time of 30.4 ± 25.9 ms.

Location of SVBNs. Based on MRI guidance and recording locations, convergence and divergence SVBNs are located throughout the cMRF, lateral to the OMN. According to May et al. (21), premotor lens accommodation neurons that are part of the near response population are located bilaterally throughout the recorded region. We plotted the location of the recorded neurons relative to the location of the lens-accommodation premotor neurons labeled following rabies injections into the ciliary body (Fig. 5). The clear overlap in the locations of these two populations reinforces the hypothesis that the recorded cells are involved in the control of the near response, and more particularly in the control of disjunctive saccades.

Discussion

The central control of binocular movements has long been debated and this discussion has crystalized into the two classic camps of eye movement control (4, 16, 18, 32–35) (Fig. 6*A*). Over a 100 y ago, Hering (33) proposed that the two eyes move in a coordinated fashion and should be seen as a single organ rather than two separate entities because they receive the same commands simultaneously. His model suggested that there are separate conjugate and vergence controllers, and that each controller sends the same command to both eyes (Fig. 6*A*). The combination of the two commands then produces the appropriate movement of the eyes to direct them at the new target location in the 3D space. However, according to Helmholtz (34), the two eyes are each directed independently at targets in 3D space (Fig. 6*A*). He proposed that binocular coordination is a learned process that gives the appearance of yoked movement, and that consequently the right eye and left eye are controlled by their own monocular neural populations, which direct them toward the target. This model eliminates the need for combining separate vergence and conjugate signals to produce disjunctive saccades.

Table 1. Summary of all SVBNs recorded

Cell	Linear sensitivity	R^2	Lead time	*FRmax*	*C*	R^2	Gaussian kernel
C1	1.78	0.84	52	443	177	0.86	20
C2	0.51	0.41	0	77	13	0.68	20
C3	1.86	0.96	22	718	295	0.96	20
C4	1.10	0.70	45	198	19	0.73	30
C5	1.29	0.94	0	800	512	0.93	20
C6	1.60	0.92	17	370	99	0.90	20
C7	0.55	0.84	78	800	1,413	0.83	10
C8	0.48	0.82	48	83	51	0.77	20
C9	0.94	0.98	59	800	775	0.98	20
D1	−0.81	0.92	28	800	948	0.92	20
D2	−0.81	0.83	60	98	53	0.86	40
D3	−1.11	0.62	9	250	148	0.64	20
D4	−1.17	0.67	0	266	142	0.67	10
D5	−1.86	0.76	16	302	89	0.80	20
D6	−0.22	0.93	6	800	3,646	0.93	20
D7	−0.19	0.49	72	39	50	0.53	20
D8	−1.48	0.88	9	800	507	0.87	20
D9	−1.89	0.88	27	262	57	0.82	20
Mean	1.09	—	30.4	—	—	—	
SD	0.57	—	25.9	—	—	—	

Column 1: Sensitivity [(spikes/second)/(degrees/second)] from linear fit of firing rate vs. vergence velocity. Population mean and SD calculated from absolute values. Column 2: Coefficient of determination of linear fit. Column 3: Lead time of firing rate vs. vergence velocity. Column 4: *FRmax* value for nonlinear fit of firing rate vs. vergence velocity. Column 5: *C* value for nonlinear fit of firing rate vs. vergence velocity. Column 6: Coefficient of determination of nonlinear fit. Column 7: Gaussian kernel bandwidth (milliseconds) used to generate spike density waveforms.

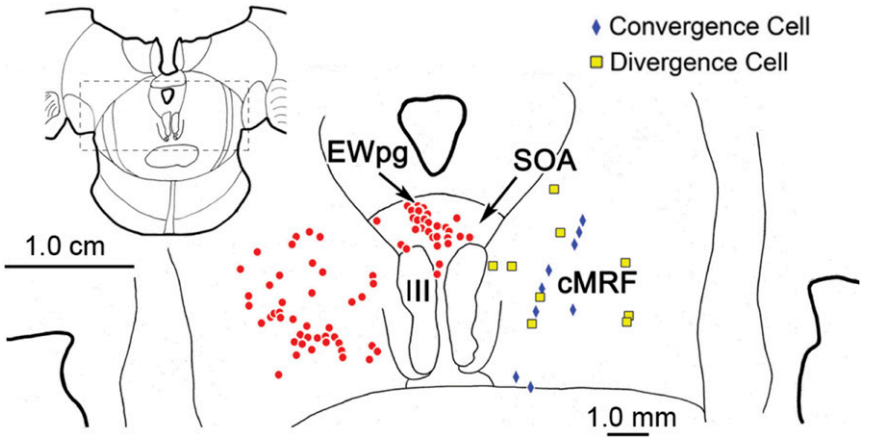

Fig. 5. Distribution of recorded saccade-vergence burst neurons (SVBNs) projected onto a single coronal section. SVBNs recorded from both the left and right cMRF were projected onto the right-hand side of the diagram for simplicity. Recordings ranged over ±3 mm in AP extent. Convergence SVBNs (blue diamonds) and divergence SVBNs (yellow squares) were intermixed within the central mesencephalic reticular formation (cMRF). SVBNs were located throughout the range of lens accommodation premotor neurons transsynaptically labeled by rabies virus (red dots) injected from the ciliary body, as illustrated on the left-hand side of the diagram [redrawn from the data in May et al. (21)]. The region shown at higher magnification is represented by the dashed rectangle in the low-magnification section. Abbreviations: III, oculomotor nucleus; cMRF, central mesencephalic reticular formation; EWpg, preganglionic Edinger–Westphal nucleus; SOA, supraoculomotor area.

In support of the Helmholtz model, some recent experiments have reported that the saccadic premotor pathway provides both the conjugate and the vergence premotor commands in order to facilitate vergence velocity during disjunctive saccades. In fact, neural recordings of excitatory burst neurons in the PPRF during disjunctive saccades showed that the firing of premotor SBNs is often correlated with only one eye or the other, so they not only carry conjugate saccade-related information, but also the vergence-related information necessary for disjunctive saccades (15, 17, 18). However, the models in which the burst generator is organized in a monocular fashion and different monocular signals are sent to the lateral rectus and the medial rectus muscles for disjunctive saccades, do not appear to account for the movement of both eyes (Fig. 6*A*). This is because AINs do not carry the appropriate signal needed to support the model from the PPRF SBNs to the contralateral MRMNs (19, 20, 36).

In contrast, based on behavioral studies in 1992, Zee et al. (4) proposed a model (Fig. 6*B*) that generated the enhanced vergence velocity observed during disjunctive saccades using the vergence subsystem, as did Busettini and Mays (6) in a 2005 model (Fig. 6*C*). The omnipause model (Fig. 6*B*) of Zee et al. proposed that omnipause neurons normally inhibit not only SBNs (37), but also SVBNs. During saccades, omnipause neurons will release their inhibition of SVBNs. SVBNs will then generate a burst of activity and consequently enhanced vergence velocity, if, and only if, a vergence motor error signal is also present. This coincidence of signals will only occur for disjunctive saccades since there is no vergence motor error signal present during conjugate saccades. Furthermore, during smooth vergence eye movements in the absence of a saccade, SVBNs will remain inhibited by omnipause neurons, and there will be no enhanced vergence velocity signal during such vergence eye movements. Under these conditions, the vergence motor error signal drives only VVNs to produce symmetrical vergence movements and, by way of the vergence integrator, to maintain vergence angle during fixation following the movement. Subsequently, Busettini and Mays (6) found, as confirmed by Kumar et al. (38), that in disjunctive saccades, vergence dynamics were influenced by versional dynamics. This resulted in the multiplicative model of Busettini and Mays (Fig. 6*C*). In this model, coincident vergence motor error signals are multiplied by saccadic burst signals to generate the SVBN signal. This occurs if, and only if, both signals are present; a condition that only occurs for disjunctive saccades; otherwise when one signal is missing, the product is zero. Specifically, this coincidence of signals will only occur for disjunctive saccades since there is no vergence motor error signal present during conjugate saccades. Furthermore, during smooth vergence eye movements in the absence of a saccade, SBNs will be silent and there will therefore be no enhanced vergence velocity signal produced. Note that in both models, vergence motor error also drives VVNs, which contribute to the vergence movement. VVN signals, along with those of the SVBNs, are integrated by the vergence position neurons in the SOA, so that vergence angle is maintained at the completion of the movement irrespective of the relative VVN and SVBN contributions. It should be noted that while both of these models predicted the characteristics of the SVBNs we have recorded, they are theoretical in nature. No model that takes into account the known cell circuitry has been proposed at present.

In 2019, Gibaldi and Banks (39) proposed a modification to the omnipause model to account for their findings that binocular eye movements are adapted to the natural environment. Their model proposes that the vergence response is based on both an estimate of target disparity, as well as disparity priors that are potentially stored and/or generated by the cerebellum. We have included their findings in the models proposed in Fig. 6 *B* and *C*. Consistent with their suggestion of a cerebellar role, previous studies have described a role for the cerebellum in the control of vergence eye movements (40, 41).

The findings described here demonstrate that the cMRF contains the previously hypothesized population of SVBNs. Furthermore, these cells display three unique characteristics that are predicted by the models described above: 1) they discharge when animals perform a disjunctive saccade, 2) they remain silent during symmetric vergence eye movements or conjugate saccades, and 3) they burst without regard to direction (rightward or leftward) of the disjunctive saccade. A recent recording study (10) characterized the vergence velocity sensitivity of cells in the SOA located dorsal and immediately lateral to the OMN. They noted a continuum of velocity sensitivities, with some cells showing little or no sensitivity and others showing considerable sensitivity. Those at the low end of the continuum would appear to be equivalent to tonic firing, near response neurons that maintain vergence angle during fixation (8). The fact that these neurons do not respond for fast intrasaccadic vergence suggests that the enhancement of vergence velocity is encoded elsewhere during disjunctive saccades

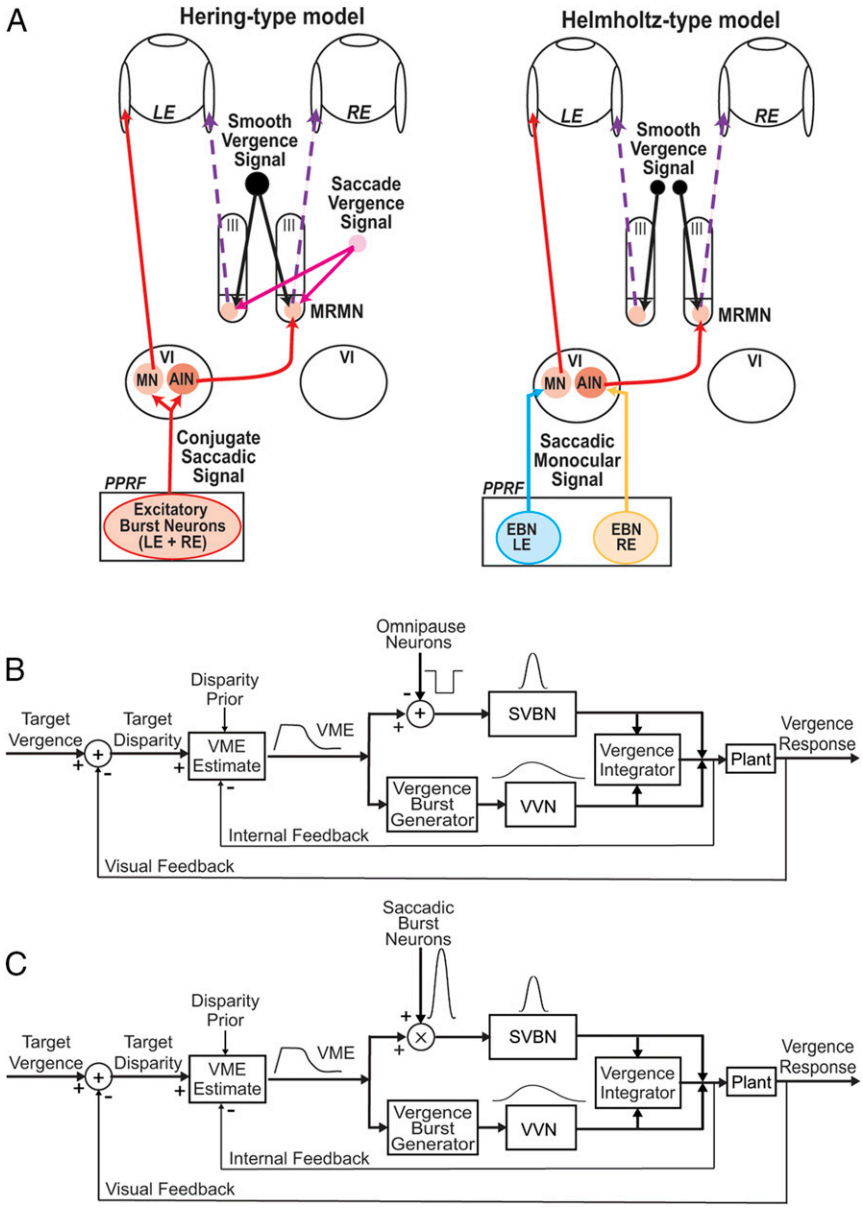

Fig. 6. (*A*) Hering-type (*Left*) and Helmholtz-type (*Right*) models proposed to explain binocular coordination of eye movements. III, oculomotor nucleus; VI, abducens nucleus; AIN, abducens internuclear neurons; EBN, excitatory burst neurons; LE, left eye; MN, motoneurons; MRMN, medial rectus motoneurons; PPRF, paramedian pontine reticular formation; RE, right eye. (*B*) Schematic for a potential model to explain the pathway involved in generating the enhanced vergence velocity signal during disjunctive saccades. Modified from Zee et al. (4). During saccades, omnipause neurons pause and release their inhibition of SVBNs. SVBNs then generate a burst of activity and consequently enhanced vergence velocity, if, and only if, a vergence motor error (VME) signal is also present. This coincidence of signals will only occur for disjunctive saccades since there is no vergence motor error signal present during conjugate saccades. Furthermore, during smooth vergence eye movements in the absence of a saccade, SVBNs will remain inhibited by omnipause neurons and there will be no enhanced vergence velocity signal during such vergence eye movements. Under these conditions, the vergence motor error signal only influences the vergence burst generator that then drives vergence velocity neurons (VVNs) to produce a symmetrical vergence movement and, by way of the vergence integrator that also receives SVBN input, to maintain vergence angle following the movement and subsequent fixation. (*C*) Schematic for a potential model to explain the pathway involved in generating the enhanced vergence velocity signal during disjunctive saccades. Modified from Busettini and Mays (6). During disjunctive saccades, the coincident vergence motor error and saccadic burst signals are multiplied to generate the SVBN signal. This coincidence of signals will only occur for disjunctive saccades since there is no vergence motor error signal present during conjugate saccades. Furthermore, during smooth vergence eye movements in the absence of a saccade, SBNs will be silent and there will be no enhanced vergence velocity signal during such vergence eye movements. Under these conditions, the vergence motor error signal only influences the vergence burst generator that then drives VVNs to produce a symmetrical vergence movement and, by way of the vergence integrator that also receives SVBN input, to maintain vergence angle during the subsequent fixation.

(10). Those cells at the high end of the continuum would appear to include burst tonic VVNs commonly found just lateral to the OMN in the medial cMRF (7). However, even the firing of these VVNs accounts for less than 10% of the increased vergence velocity during disjunctive saccades (10). Thus, it seems reasonable to propose that the remaining >90% of the increased vergence speed observed for disjunctive saccades is encoded by the SVBNs in the cMRF.

Our results demonstrate a clear role of cMRF in the control of disjunctive saccades. This represents an expansion in the functions

of this region. Numerous studies have shown its role in conjugate saccades. Indeed, Cohen et al. (24, 25) showed that electrical stimulation of the cMRF evoked contraversive horizontal conjugate saccades, and many cMRF neurons fire before or during conjugate saccades (26, 42, 43). More recently, Waitzman et al. (29) reported that disconjugate eye movements can be elicited from some cMRF sites, suggesting its involvement in disjunctive saccades. Anatomical work indicates the cMRF projects bilaterally to MRMNs and the abducens nucleus (23, 44, 45), suggesting that SVBNs are likely to have the appropriate connections to directly activate motoneurons. Furthermore, the location of the SVBNs in the cMRF places them within a dense field of collicular terminals contributed by predorsal bundle axon collaterals (46–49), a likely source of saccadic signals. A cMRF projection to the SOA is also present (27). This likely includes a projection by SVBNs, and not just VVNs, indicating that the former also access the vergence integrator. Our recent studies, in which rabies virus was injected into the ciliary muscle in monkeys, indicate that the cMRF does indeed contain premotor neurons that supply EWpg motoneurons bilaterally (21). Thus, SVBNs could play a role in all of the components of near triad responses.

The source of the proposed vergence motor error information is currently unknown. One potential pathway goes through the cerebellum by way of the nucleus reticularis tegmenti pontis (NRTP). The caudal portion of the NRTP contains neurons that carry signals related to conjugate saccades, vergence (near- and far-response activity) and lens accommodation (50). They are characterized by a burst-tonic increase in firing rate, but they have not been tested for disjunctive saccades (50). When animals perform symmetrical vergence movements, without a saccade, the firing rate of many of these neurons is correlated with both vergence position and velocity. The close proximity of saccade-related and vergence neurons suggests that some saccade-related cells could be tuned in depth and, considering its connections, the NRTP is in a position to supply the cerebellum with crucial information related to the location of targets in 3D space. Indeed, the caudal fastigial nucleus and posterior interposed nucleus have been shown to be involved in vergence movements and lens accommodation in normal (40, 51, 52) and strabismic monkeys (13). The caudal fastigial nucleus contains near-response neurons (51, 52), as well as saccade-related neurons (53), and it projects directly to SBNs in the PPRF (54), whereas the posterior interposed nucleus contains far-response neurons, as well as neurons whose responses are related to disparity information (40). Consequently, Zhang and Gamlin (51) proposed that these two nuclei interact in a push–pull system for modulating vergence and lens accommodation. Both these nuclei also project to the SOA (41) and may play a role in the control of tonic near response neurons. It remains to be determined whether they also project to the cMRF where SVBNs are located.

In summary, our findings propose that cMRF cells, and SVBNs in particular, play a critical role in the control of disjunctive saccades. Further studies of disjunctive saccades in brain areas that might supply input to SVBNs are required for further understanding of the circuits that control these eye movements, which are critical for viewing targets in 3D space, to explain and advance solutions that could treat strabismus.

Methods

Subjects and Surgical Procedure. Two adult male rhesus macaque monkeys (*Macaca mulatta*) were used in this study. All experimental procedures were approved by the University of Alabama Institutional Animal Care and Use Committee and complied with the US Public Health Service Policy on Humane Care and Use of Laboratory Animals. All surgical procedures were performed under sterile conditions using general anesthesia (isoflurane). Postsurgically, animals received analgesics to minimize pain and antibiotics to prevent infection. Each animal underwent three surgeries. Initially, two polyether ether ketone (PEEK) fixation plates attached to the skull by bone screws were implanted. Once the bone healed, a search coil was implanted on each eye under the conjunctiva (55). These devices allowed us to record the movement of both eyes with high accuracy. At the same time, four PEEK fixation struts were attached onto the plates already secured to the skull of the animal. A headpost was centered and cemented between the fixation plates with dental acrylic. With this system, the head can be held fixed during training and recording sessions. After full recovery from surgery, monkeys were trained on visual tasks. Then, both animals underwent an MRI procedure, using a Siemens Prisma 3.0T whole-body MRI with a magnetization-prepared rapid acquisition with gradient echo structural sequence at 0.8-mm isotropic resolution. During the imaging, a fiducial array was attached to the PEEK fixation plates to enable later localization of structures of interest. Finally, two recording cylinders (16-mm diameter) were implanted over a craniotomy on each side of the skull. Placement of chambers and targeting of electrodes to the cMRF were performed using MRI guidance from a Brainsight navigation system (Rogue Research).

Eye Movement Recording and Visual Display. Both animals were trained to perform several different visual tasks. During the training and experimental sessions, monkeys were seated in a primate chair with their head restrained, and placed in the middle of a magnetic field, while they were positioned on a fixed table. They faced a projection screen (90° × 70°) located at a viewing distance of 95 cm. The fixation target was a white dot (0.7° diameter) over a gray background projected from a projector (Epson PowerLite 485W; 1,280 × 800). This display was used to elicit all conjugate and some disjunctive saccades. A green light-emitting diode (LED), mounted on a vertically adjustable beam attached to a motor-driven platform (Newmark X-Y linear stage; CS Series Belt Drive) was positioned horizontally over a range of ±25° to elicit the horizontal component of disjunctive eye movements. This LED could also be moved along the beam over a range of vergence angle (2 to 12°) to elicit the vergence component of the disjunctive eye movements. When placed immediately in front of the animal's midline, this target was used to elicit symmetric vergence.

Monkeys were trained to look at a visual target for a water reward. An audible tone signaled trial initiation. All trials began with the appearance of a fixation target, which the monkey was required to fixate for 1,500 to 2,000 ms (randomized duration). At the end of the fixation time, the target was extinguished and at the same time, a peripheral target appeared. Depending on the type of trial, this was either a target on the tangent screen or the illuminated LED. The different trial types were pseudorandomized throughout the experiment. To generate disjunctive saccades, the required eye movement was either from the tangent screen to a near LED to elicit a convergence movement, or vice versa to generate a divergence movement.

Eye movements were measured with a phase-angle detection system (Riverbend system) and voltage signals encoding the horizontal and vertical positions of the eye were sampled at 1 kHz. Each eye coil signal was calibrated independently by having the monkey fixate visual targets located at different eccentricities (up to ±16° in 2° horizontal steps and up to ±12° by steps of 2° vertically) on the tangent screen. The data acquisition, the online control of the oculomotor task, and the triggering of visual stimuli were all controlled using a real-time Linux computer.

Behavioral Tasks. To test the characteristics of each neuron in the cMRF, monkeys had to perform several different eye movement tasks (Fig. 1).

Saccadic trials. Animals were required to make saccades toward visual targets (fixation and peripheral) located on the tangent screen in front of them. The range of target locations was up to ±16° in 2° horizontal steps, and 0°, ±4°, ±10°, and ±12°, vertically. Each of the target locations were chosen randomly. Thus, this trial type required the animal to make a conjugate saccade without vergence.

Symmetrical vergence pursuit trials. Animals were required to make smooth symmetrical vergence pursuit eye movements by following the LED apparatus aligned with the animal's midsagittal plane. The LED approached the animal (convergence or near-response eye movement) or receded (divergence or far-response eye movement). The desired vergence angle varied from 2 to 12°. Thus, this trial type required the animal to make a vergence eye movement without a saccade.

Disjunctive trials. Animals were required to make disjunctive eye movements by looking at a target stepped from straight-ahead on the tangent screen to the LED located at a closer distance and at a different horizontal position (near disjunctive eye movements requiring convergence and designated as a positive vergence angle), or by looking from the LED toward a target at a different horizontal location on the tangent screen (far disjunctive eye movements requiring divergence and designated as a negative vergence angle). Thus, this trial type required the animal to make a disjunctive saccade with both vergence and conjugate components, akin to most natural eye movements.

Unit Recording and Localization. Tungsten microelectrodes (Microprobe; 0.7 to 1.0 MΩ) were used to record extracellular activity from the SOA and the cMRF. The OMN was first defined by its high-frequency tonic firing rate and contralateral burst-tonic activity during conjugate saccades. The SOA is located immediately dorsal to the OMN. As reported by Mays (8), cells in this area commonly discharge with a tonic firing rate when monkeys perform symmetrical vergence eye movements. The microelectrode was moved laterally from these structures, up to 5 mm from the lateral border of the OMN, to characterize the cMRF. Saccadic neurons, as previously described (24, 26, 42, 43), were encountered in this area, as well as vergence-related neural activity. The SVBNs that were the target of this study were relatively infrequently encountered and were distributed widely within the recording coordinates. In fact, only 18 SVBNs were encountered among 172 cells with vergence-related activity; but as these cells are silent during both fixation and conjugate activity, they are challenging to find. Preliminary detection of spikes was performed online, with unit activity filtered at 5 kHz and the occurrence of spikes detected by a window discriminator.

Data Analysis. Experimental control and data acquisition were accomplished by a Linux computer using software for data visualization and storage. Offline analysis was performed in MATLAB (Mathworks) using custom software. All eye movement data were additionally calibrated offline, and movement onsets and offsets were manually identified based on velocity traces. Raw spike data were acquired at a sampling rate of 25 kHz. Spike times were converted to spike density functions by convolving them with a Gaussian kernel having a bandwidth of 10 to 40 ms, and optimized to the cell firing rate (56, 57). Horizontal version was computed as the average of right eye and left eye position. Horizontal vergence position (VA) was calculated as the difference between right eye and left eye positions. Velocities were computed using a 3-points differentiation.

For the models discussed in *Results*, multiple linear regression was used to estimate neuronal sensitivity of the parameters using nonparametric bootstrapping with 2,000 iterations (30). CIs of each parameter were determined by the bias-corrected and accelerated method. This procedure allowed us to determine which monocular (left or right eye) parameters could be replaced with binocular parameters, either conjugate or vergence, by checking for CI overlap in the same or opposing directions. Overlap with zero indicates that a parameter can be eliminated without significantly decreasing predictive power. To assess the fit of the models, we used the measure of VAF, which has been used in previous studies with the same approach (20, 58), and is calculated as 1 minus the ratio of the variance of the estimated firing rate to the actual firing rate. This is analogous to the coefficient of determination (R^2) also used in this study. For each cell, a single delay was added to account for the time between firing rate and the subsequent associated eye movement response to give the best overall fits, determined systematically by running the saturation model at different latencies. For a given cell, the same delay was used for all trials and model fits. For the saturation model, the *FRmax* parameter was not allowed to exceed 800. Beyond this number, the fitting algorithm gave biologically unmeaningful numbers to force the model to fit essentially linear data. After models were assigned, parameter estimations were produced by nonlinear least-squares curve fitting in Matlab 2020a. To analyze trials with conjugate saccades and smooth symmetrical vergence eye movements, identical kernel bandwidths were used. Conjugate saccades were divided into leftward and rightward saccades, whereas symmetric eye movements were divided into divergence and convergence smooth vergence. For saccadic trials, only those with a vergence landing error of less than 1° were considered.

Data Availability. Data used in the production of this paper have been deposited in the Open Science Framework database, https://osf.io/ny2s5/ (DOI: 10.17605/OSF.IO/NY2S5) (59).

ACKNOWLEDGMENTS. This work was supported by NIH/National Eye Institute Grants EY014263 and EY003039, and by Research to Prevent Blindness. We thank Dr. Claudio Busettini for his comments and suggestions on the models describing the generation of disjunctive saccades. We also thank Julie Hill, Debbie Whitten, Samuel Hayley, Mark Bolding, and Eric Worthington for their technical assistance.

1. R. J. Leigh, D. S. Zee, *The Neurology of Eye Movements* (Oxford University Press, 2015).
2. H. Ono, S. Nakamizo, M. J. Steinbach, Nonadditivity of vergence and saccadic eye movement. *Vision Res.* **18**, 735–739 (1978).
3. J. T. Enright, Changes in vergence mediated by saccades. *J. Physiol.* **350**, 9–31 (1984).
4. D. S. Zee, E. J. Fitzgibbon, L. M. Optican, Saccade-vergence interactions in humans. *J. Neurophysiol.* **68**, 1624–1641 (1992).
5. L. E. Mays, P. D. Gamlin, Neuronal circuitry controlling the near response. *Curr. Opin. Neurobiol.* **5**, 763–768 (1995).
6. C. Busettini, L. E. Mays, Saccade-vergence interactions in macaques. II. Vergence enhancement as the product of a local feedback vergence motor error and a weighted saccadic burst. *J. Neurophysiol.* **94**, 2312–2330 (2005).
7. L. E. Mays, J. D. Porter, P. D. Gamlin, C. A. Tello, Neural control of vergence eye movements: Neurons encoding vergence velocity. *J. Neurophysiol.* **56**, 1007–1021 (1986).
8. L. E. Mays, Neural control of vergence eye movements: Convergence and divergence neurons in midbrain. *J. Neurophysiol.* **51**, 1091–1108 (1984).
9. S. J. Judge, B. G. Cumming, Neurons in the monkey midbrain with activity related to vergence eye movement and accommodation. *J. Neurophysiol.* **55**, 915–930 (1986).
10. A. C. Pallus, M. M. G. Walton, M. J. Mustari, Response of supraoculomotor area neurons during combined saccade-vergence movements. *J. Neurophysiol.* **119**, 585–596 (2018).
11. V. E. Das, Strabismus and the oculomotor system: Insights from macaque models. *Annu. Rev. Vis. Sci.* **2**, 37–59 (2016).
12. M. M. Walton, M. J. Mustari, Abnormal tuning of saccade-related cells in pontine reticular formation of strabismic monkeys. *J. Neurophysiol.* **114**, 857–868 (2015).
13. A. C. Joshi, V. E. Das, Muscimol inactivation of caudal fastigial nucleus and posterior interposed nucleus in monkeys with strabismus. *J. Neurophysiol.* **110**, 1882–1891 (2013).
14. V. E. Das, Responses of cells in the midbrain near-response area in monkeys with strabismus. *Invest. Ophthalmol. Vis. Sci.* **53**, 3858–3864 (2012).
15. K. E. Cullen, M. R. Van Horn, The neural control of fast vs. slow vergence eye movements. *Eur. J. Neurosci.* **33**, 2147–2154 (2011).
16. W. M. King, Binocular coordination of eye movements—Hering's law of equal innervation or uniocular control? *Eur. J. Neurosci.* **33**, 2139–2146 (2011).
17. W. Zhou, W. M. King, Premotor commands encode monocular eye movements. *Nature* **393**, 692–695 (1998).
18. M. R. Van Horn, P. A. Sylvestre, K. E. Cullen, The brain stem saccadic burst generator encodes gaze in three-dimensional space. *J. Neurophysiol.* **99**, 2602–2616 (2008).
19. P. D. Gamlin, J. W. Gnadt, L. E. Mays, Abducens internuclear neurons carry an inappropriate signal for ocular convergence. *J. Neurophysiol.* **62**, 70–81 (1989).
20. P. A. Sylvestre, K. E. Cullen, Dynamics of abducens nucleus neuron discharges during disjunctive saccades. *J. Neurophysiol.* **88**, 3452–3468 (2002).
21. P. J. May, I. Billig, P. D. Gamlin, J. Quinet, Central mesencephalic reticular formation control of the near response: Lens accommodation circuits. *J. Neurophysiol.* **121**, 1692–1703 (2019).
22. P. J. May, S. Warren, M. O. Bohlen, M. Barnerssoi, A. K. Horn, A central mesencephalic reticular formation projection to the Edinger-Westphal nuclei. *Brain Struct. Funct.* **221**, 4073–4089 (2016).
23. M. O. Bohlen, S. Warren, P. J. May, A central mesencephalic reticular formation projection to medial rectus motoneurons supplying singly and multiply innervated extraocular muscle fibers. *J. Comp. Neurol.* **525**, 2000–2018 (2017).
24. B. Cohen, D. M. Waitzman, J. A. Büttner-Ennever, V. Matsuo, Horizontal saccades and the central mesencephalic reticular formation. *Prog. Brain Res.* **64**, 243–256 (1986).
25. B. Cohen, V. Matsuo, J. Fradin, T. Raphan, Horizontal saccades induced by stimulation of the central mesencephalic reticular formation. *Exp. Brain Res.* **57**, 605–616 (1985).
26. D. M. Waitzman, V. L. Silakov, B. Cohen, Central mesencephalic reticular formation (cMRF) neurons discharging before and during eye movements. *J. Neurophysiol.* **75**, 1546–1572 (1996).
27. M. O. Bohlen, S. Warren, P. J. May, A central mesencephalic reticular formation projection to the supraoculomotor area in macaque monkeys. *Brain Struct. Funct.* **221**, 2209–2229 (2016).
28. J. Quinet, K. Schultz, P. J. May, P. D. Gamlin, Are there distinct roles for SOA and cMRF premotor neurons in disconjugate eye movements in the primate? *Soc. Neurosci. Abstr.* **43**, 150.06 (2017).
29. D. M. Waitzman, M. R. Van Horn, K. E. Cullen, Neuronal evidence for individual eye control in the primate cMRF. *Prog. Brain Res.* **171**, 143–150 (2008).
30. J. Carpenter, J. Bithell, Bootstrap confidence intervals: When, which, what? A practical guide for medical statisticians. *Stat. Med.* **19**, 1141–1164 (2000).
31. J. A. Van Gisbergen, D. A. Robinson, S. Gielen, A quantitative analysis of generation of saccadic eye movements by burst neurons. *J. Neurophysiol.* **45**, 417–442 (1981).
32. P. D. Gamlin, Subcortical neural circuits for ocular accommodation and vergence in primates. *Ophthalmic Physiol. Opt.* **19**, 81–89 (1999).
33. E. Hering, *The Theory of Binocular Vision*, B. Bridgeman, L. Stark, Eds. (Plenum, New York, 1977) [originally published as *Die Lehre vom binokularen Sehen* (Engelmann, Leipzig, 1868); translated by B. Bridgeman].
34. H. Helmholtz, *Helmholtz's Treatise on Physiologica Optics* (Dover, New York, 1962).
35. W. M. King, W. Zhou, Neural basis of disjunctive eye movements. *Ann. N. Y. Acad. Sci.* **956**, 273–283 (2002).
36. J. M. Miller, R. C. Davison, P. D. Gamlin, Motor nucleus activity fails to predict extraocular muscle forces in ocular convergence. *J. Neurophysiol.* **105**, 2863–2873 (2011).
37. C. A. Scudder, C. S. Kaneko, A. F. Fuchs, The brainstem burst generator for saccadic eye movements: A modern synthesis. *Exp. Brain Res.* **142**, 439–462 (2002).
38. A. N. Kumar *et al.*, Tests of models for saccade-vergence interaction using novel stimulus conditions. *Biol. Cybern.* **95**, 143–157 (2006).
39. A. Gibaldi, M. S. Banks, Binocular eye movements are adapted to the natural environment. *J. Neurosci.* **39**, 2877–2888 (2019).
40. H. Zhang, P. D. Gamlin, Neurons in the posterior interposed nucleus of the cerebellum related to vergence and accommodation. I. Steady-state characteristics. *J. Neurophysiol.* **79**, 1255–1269 (1998).

41. P. J. May, J. D. Porter, P. D. Gamlin, Interconnections between the primate cerebellum and midbrain near-response regions. *J. Comp. Neurol.* **315**, 98–116 (1992).
42. J. A. Cromer, D. M. Waitzman, Neurones associated with saccade metrics in the monkey central mesencephalic reticular formation. *J. Physiol.* **570**, 507–523 (2006).
43. J. A. Cromer, D. M. Waitzman, Comparison of saccade-associated neuronal activity in the primate central mesencephalic and paramedian pontine reticular formations. *J. Neurophysiol.* **98**, 835–850 (2007).
44. W. Graf, N. Gerrits, N. Yatim-Dhiba, G. Ugolini, Mapping the oculomotor system: The power of transneuronal labelling with rabies virus. *Eur. J. Neurosci.* **15**, 1557–1562 (2002).
45. G. Ugolini *et al*., Horizontal eye movement networks in primates as revealed by retrograde transneuronal transfer of rabies virus: Differences in monosynaptic input to "slow" and "fast" abducens motoneurons. *J. Comp. Neurol.* **498**, 762–785 (2006).
46. B. Chen, P. J. May, The feedback circuit connecting the superior colliculus and central mesencephalic reticular formation: A direct morphological demonstration. *Exp. Brain Res.* **131**, 10–21 (2000).
47. A. Grantyn, R. Grantyn, Axonal patterns and sites of termination of cat superior colliculus neurons projecting in the tecto-bulbo-spinal tract. *Exp. Brain Res.* **46**, 243–256 (1982).
48. A. K. Moschovakis, A. B. Karabelas, S. M. Highstein, Structure-function relationships in the primate superior colliculus. I. Morphological classification of efferent neurons. *J. Neurophysiol.* **60**, 232–262 (1988A).
49. A. K. Moschovakis, A. B. Karabelas, S. M. Highstein, Structure-function relationships in the primate superior colliculus. II. Morphological identity of presaccadic neurons. *J. Neurophysiol.* **60**, 263–302 (1988B).
50. P. D. Gamlin, R. J. Clarke, Single-unit activity in the primate nucleus reticularis tegmenti pontis related to vergence and ocular accommodation. *J. Neurophysiol.* **73**, 2115–2119 (1995).
51. H. Zhang, P. D. Gamlin, Single unit activity within the posterior fastigial nucleus during vergence and accommodation in the alert primate. *Soc. Neurosci. Abstr.* **22**, 2034 (1996).
52. H. Zhang, P. D. Gamlin, Sensorimotor characteristics of far response neurons in the cerebellum of the rhesus monkey. *Assoc. Res. Vis. Ophthalmol.* **35**, 1282 (1994).
53. A. F. Fuchs, F. R. Robinson, A. Straube, Role of the caudal fastigial nucleus in saccade generation. I. Neuronal discharge pattern. *J. Neurophysiol.* **70**, 1723–1740 (1993).
54. P. J. May, R. Hartwich-Young, J. Nelson, D. L. Sparks, J. D. Porter, Cerebellotectal pathways in the macaque: Implications for collicular generation of saccades. *Neuroscience* **36**, 305–324 (1990).
55. S. J. Judge, B. J. Richmond, F. C. Chu, Implantation of magnetic search coils for measurement of eye position: An improved method. *Vision Res.* **20**, 535–538 (1980).
56. B. J. Richmond, L. M. Optican, H. Spitzer, Temporal encoding of two-dimensional patterns by single units in primate primary visual cortex. I. Stimulus-response relations. *J. Neurophysiol.* **64**, 351–369 (1990).
57. E. Parzen, On estimation of a probability density function and mode. *Ann. Math. Stat.* **33**, 1065–1076 (1962).
58. M. R. Van Horn, D. M. Waitzman, K. E. Cullen, Vergence neurons identified in the rostral superior colliculus code smooth eye movements in 3D space. *J. Neurosci.* **33**, 7274–7284 (2013).
59. J. Quinet, K. Schultz, P. J. May, P. D. Gamlin, Neural control of rapid binocular eye movements: Saccade-vergence burst neurons. Open Science Framework. https://osf.io/ny2s5/. Accessed 2 October 2020.
60. C. M. Schor, J. S. Maxwell, S. B. Stevenson, Isovergence surfaces: The conjugacy of vertical eye movements in tertiary positions of gaze. *Ophthalmic Physiol. Opt.* **14**, 279–286 (1994).
61. B. T. Backus, M. S. Banks, R. van Ee, J. A. Crowell, Horizontal and vertical disparity, eye position, and stereoscopic slant perception. *Vision Res.* **39**, 1143–1170 (1999).